



**HAL**  
open science

## Enhancement of absorption efficiency for a laminar film flow by hydrodynamic conditions generated by a new type of column wall

Stéphane Negny, Michel Meyer, Michel Prevost

► **To cite this version:**

Stéphane Negny, Michel Meyer, Michel Prevost. Enhancement of absorption efficiency for a laminar film flow by hydrodynamic conditions generated by a new type of column wall. *Chemical Engineering Journal*, 2001, 8 (1), pp.7-13. 10.1016/S1385-8947(00)00189-3 . hal-03604741

**HAL Id: hal-03604741**

**<https://hal.science/hal-03604741>**

Submitted on 10 Mar 2022

**HAL** is a multi-disciplinary open access archive for the deposit and dissemination of scientific research documents, whether they are published or not. The documents may come from teaching and research institutions in France or abroad, or from public or private research centers.

L'archive ouverte pluridisciplinaire **HAL**, est destinée au dépôt et à la diffusion de documents scientifiques de niveau recherche, publiés ou non, émanant des établissements d'enseignement et de recherche français ou étrangers, des laboratoires publics ou privés.

# Enhancement of absorption efficiency for a laminar film flow by hydrodynamic conditions generated by a new type of column wall

S. Negny\*, M. Meyer, M. Prevost

UMR 5503 INP-ENSIGC/CNRS, Groupe Séparation Gaz-Liquide, 18 Chemin de la Loge, 31 078 Toulouse Cedex 04, France

---

## Abstract

A numerical model is developed to quantify the effects of hydrodynamics on heat and mass transfer during an absorption, for a laminar film flowing over a wavy wall column. First of all, the modelling is written for a single wave of the wall shape. Then, an experimental set up, composed of a CCD video camera, validates this model. Finally, the model is extended to an entire column. The results include a comparison with the simulation of a smooth column having the same geometrical and operating conditions. The wavy column dissipates more heat through the wall (43%) due to the presence of a vortex in the furrows. This leads to an increase of the absorption rate at the interface (10%). Moreover, the wavy column reaches equilibrium more rapidly in spite of a lower mean film temperature.

*Keywords:* Laminar flow; Wavy wall column; Vortex

---

## 1. Introduction

The flow of liquids in thin films is a widely natural occurring phenomena, as well as in many chemical engineering operations. Fluid motion in free liquid films has become a popular means of transferring heat and mass from a vapour phase to a liquid film. Vertically falling films along a solid wall are often encountered in many industrial applications: steam condensers, evaporators, wetted wall columns, absorbers in heat pumps and gas treatment, reactors, etc. The rates of transfer of heat and mass, in both liquid and gas phases, are usually related to the film flow pattern. Therefore, many investigators search new ways to obtain hydrodynamical conditions able to enhance transfer through the films, due to their weak performance in the laminar flow range. Thus, new wall structures appear, in order to increase transfer without enhancing apparatus size. These structures consist of a deformation of the solid wall curvature and are called corrugated surfaces. Numerous types of corrugated surface exist [1]. The wavy surface is one of these corrugated structures which offers a greater film stability.

It is the purpose of the present project to study film flow patterns of a falling film flowing over a wavy wall, and to establish the relationship between hydrodynamics and the associated transfer phenomena. Firstly, a model has been developed in order to simulate the fluid flow and the

simultaneous heat and mass transfer for one furrow of the wall without the effect of gas contribution. Various fluid mechanics software packages have been tested but have not given satisfactory results, due to the vertically free gas-liquid interface. It is for this reason that we have decided to develop our own model. This model is characterised by the coupling between a detailed description of the film flow pattern with a free interface and the simultaneous heat and mass transfer. The model takes into account the current orientation taken in chemical engineering, and more precisely in the gas-liquid separation domain. Indeed, it consists of introducing the flow pattern in the determination of the simultaneous transfers. This way to proceed allows us to avoid heat and mass transfer coefficients. The numerical investigation is performed for the wavy wall column to quantify the contribution of such a surface in heat and mass transfer processes. The model is applied to the case of absorption of sulfur dioxide by a falling film of tetraethylen glycol dimethyl ether (E181). These non-conventional constituents are selected for an industrial requirement, the treatment of atmospheric rejects. The E181 has a high solubility with respect to SO<sub>2</sub> [2], which explains our choice.

## 2. Modelling for one wave

The main goal of this part is to propose a model in order to simulate hydrodynamics, heat and mass transfer for a falling film with a free interface flowing over one furrow of the column. Due to the difficulty of this purpose, modelling is

---

\* Corresponding author. Tel.: +33-5-62-25-23-00.  
E-mail address: michel.meyer@ensigct.fr (S. Negny).

## Nomenclature

|                      |  |
|----------------------|--|
| $a$                  | wave amplitude (m)   |
| $c$                  | concentration (mol/m <sup>3</sup> )  |
| $D$                  | diffusion coefficient (m <sup>2</sup> /s)                                  |
| $D_m$                | mean diameter (m)  |
| $D_p$                | wall diameter (m)  |
| $h_{ci}$             | interfacial mass transfer coefficient for the wavy tube (m/s)              |
| $h_{ci}^0$           | interfacial mass transfer coefficient for the smooth tube (m/s)            |
| $h_e$                | experimental film thickness (m)  |
| $h_t$                | theoretical film thickness (m)   |
| $h_{tp}$             | wall heat transfer coefficient for the wavy surface (w/m <sup>2</sup> K)   |
| $h_{tp}^0$           | wall heat transfer coefficient for the smooth surface (w/m <sup>2</sup> K) |
| $H$                  | molar enthalpy (J/mol)   |
| $j$                  | number of components   |
| $J$                  | molar rate (mol/m <sup>2</sup> s)  |
| $N_r^j$              | radial mass transfer rate of component $j$ (mol/m <sup>2</sup> s)          |
| $Nu$                 | mean Nusselt number for wavy tube $Nu=h_{tp}D_p/\lambda$                   |
| $Nu0$                | Nusselt number for smooth tube $Nu0=h_{tp}^0D_m/\lambda$                   |
| $N_z^j$              | axial mass transfer rate of component $j$ (mol/m <sup>2</sup> s)           |
| $p$                  | wavelength (m)   |
| $P$                  | pressure (Pa)  |
| $q_r$                | radial heat transfer (J/m <sup>2</sup> s)                                  |
| $q_z$                | axial heat transfer (J/m <sup>2</sup> s)                                   |
| $r$                  | radial component (m)   |
| $r_i$                | interfacial radius (m)   |
| $r_m$                | mean radius (m)  |
| $r_p$                | wall radius (m)  |
| $Re$                 | Reynolds number $Re=4\Gamma/\mu$   |
| $Sh$                 | mean Sherwood number for wavy tube $Shl=h_{ci}D_p/D$                       |
| $Sh0$                | Sherwood number for smooth tube $Sh0=h_{ci}^0D_m/D$                        |
| $T$                  | temperature (K)  |
| $v_r$                | radial velocity (m/s)  |
| $v_z$                | axial velocity (m/s)   |
| $X_{SO_2}$           | mean liquid molar fraction in SO <sub>2</sub>                              |
| $z$                  | axial component (m)  |
| <i>Greek symbols</i> |  |
| $\psi$               | stream function  |
| $\omega$             | vorticity  |
| $\xi$                | axial component in the mathematical domain                                 |
| $\eta$               | radial component in the mathematical domain                                |
| $\sigma$             | surface tension (N/m)  |
| $\nu$                | dynamic viscosity (m <sup>2</sup> /s)                                      |
| $\lambda$            | heat conduction coefficient (J/m s K)                                      |

|          |  |
|----------|--|
| $\Gamma$ | Mass flow rate divided by the wetted perimeter (kg/m <sup>2</sup> s) |
| $\rho$   | liquid density (kg/m <sup>3</sup> )                                  |
| $\mu$    | liquid viscosity (Pa s)  |

### Mathematical operators

$$\nabla^2 = \frac{\partial^2}{\partial r^2} - \frac{1}{r} \frac{\partial}{\partial r} + \frac{\partial^2}{\partial z^2}$$

achieved according to a sequential approach: hydrodynamics then heat and mass transfer. Firstly, the hydrodynamics model is investigated and the velocity fields obtained as a result are incorporated in the second part which consists of modelling the simultaneous heat and mass transfer. By the introduction of the velocity, the heat and mass transfer coefficients are avoided and the narrow link between motion and transfer can be studied. The entire modelling is dedicated to the liquid phase in order to analyse the contribution of a wavy surface on the liquid phase alone. The gas phase is supposed to be stagnant. Other assumptions are that the flow is readily established and as the wall shape is periodical the modelling is reduced to one furrow.

### 2.1. Hydrodynamics

The fluid falling over the surface is considered Newtonian, laminar, incompressible and isothermal. For the theoretical model, the Navier–Stokes equations are used for the bulk of the film and a specific equation for the interface position. The formulation of the Navier–Stokes equations is expressed in terms of stream function and vorticity. The principal difficulty of this part is that the interface is free, that is it is able to move. The interface position is reached by an equation based on a force balance and under the following assumptions: no ripples, constant surface tension, constant gas pressure. The demonstration which leads to this equation is very long and arduous, further details are given by [3]. Finally, the theoretical description leads to the following system:

$$\begin{cases} -\frac{1}{r} \frac{\partial (\psi, \omega)}{\partial (r, z)} - \frac{2}{r^2} \frac{\partial \psi}{\partial z} \omega = \nu \nabla^2 \omega \\ \omega = \nabla^2 \psi \\ r_i^2 \left( \frac{d^3 r_i}{dz^3} - \frac{1}{\sigma} \frac{\partial P}{\partial z} \right) + \frac{dr_i}{dz} = 0 \text{ (interface equation)} \end{cases} \quad (1)$$

Concerning boundary conditions, no slip conditions are expressed at the wall, continuity of the tangential velocity at the interface. As the wall shape is sinusoidal, periodic conditions are also added. Some precisions on this model are given in [4].

### 2.2. Heat and mass transfer

This part is dedicated to the second part of the entire model: the simultaneous heat and mass transfer for a

multicomponent mixture. As we mentioned before, the velocity fields are included in the transfer rates as follows:

$$N_k^j = v_k c^j + J_k \quad (2)$$

$$q_k = \sum_j N_k^j H^j - \lambda \frac{\partial T}{\partial k}, \quad k = r, z \quad (3)$$

The heat and mass transfer are clearly coupled because the heat rates are expressed with the mass rates, and heat conduction and mass diffusion coefficients are both temperature and concentration dependent. The enthalpy term is calculated by the use of a thermodynamic software package Prophy [5]. Prophy is a general software package which widely covers the thermodynamic properties of a component or a mixture, for various thermodynamic models.

The axial diffusion term for mass transfer and the axial conduction term for heat transfer are neglected with respect to the transport term. To express diffusion, two laws can be used: the Fick's law and the Maxwell Stephan one [6]. In order to have the same number of equations and unknowns, two classical rate balance equations are added:

$$\frac{\partial N_z^j}{\partial z} + \frac{N_r^j}{r} + \frac{\partial N_r^j}{\partial r} = 0 \quad (4)$$

$$\frac{\partial q_z^j}{\partial z} + \frac{q_r^j}{r} + \frac{\partial q_r^j}{\partial r} = 0 \quad (5)$$

Concerning boundary conditions, the inlet rates are supposed to be known, the wall temperature is kept constant and equilibrium is reached at the interface.

### 2.3. Resolution

Equations of both systems (hydrodynamic and transfer) are discretised, however, the physical domain does not have rectangular coordinates. The algebraic transformation used by [7] is extended for our problem:  $\eta = r - r_i/r_p - r_i$ ,  $\xi = z$ , Fig. 1. It allows to map the physical complex domain onto a rectangular mathematical one. All equations are translated and discretised in this new domain. For both systems, the discretisation step leads to a system of non linear algebraic equations. For each system, all equations are solved simultaneously by an iterative Newton–Raphson method. At each iteration a linear system is solved, and the Jacobian matrix

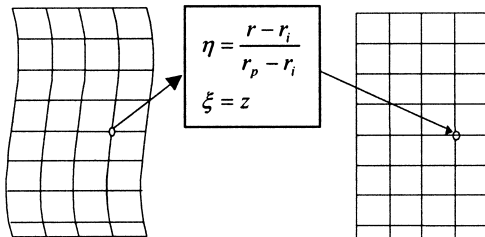


Fig. 1. Algebraic transformation.

is analytically evaluated. Nevertheless, a judicious arrangement of equations and variables gives a tridiagonal bloc Jacobian matrix for the hydrodynamical model and a bidiagonal one for the transfer model. In order to decrease the CPU time, these particular structures are exploited in the resolution.

The principal inconvenience of the Newton–Raphson method is that it is locally convergent, initialisation is therefore an important point. Thus, for a fixed Reynolds number, the results of the smooth tube initialise the simulation and the wave amplitude is gradually increased, i.e. is used as a homotopic parameter. Each time, the initialisation is performed with the results of the preceding wave amplitude. The resolution is decomposed in two steps corresponding to those of the model: hydrodynamics followed by transfer.

### 2.4. Results

To more easily understand the results for an entire column, a summary on hydrodynamics, heat and mass transfer results is given for a single furrow (for further details refer to [8]). In this part, the liquid is pure and its temperature is 293 K at the inlet. The gas phase is pure and at the same temperature. The wall temperature is constant, at 293 K, all along the furrow. During the laminar flow regime, the particular structure of the wall shape drives to the appearance of a vortex in the second part of the furrow. A reversed flow is created near the wall. The vortex arises for a Reynolds number around 15, Fig. 2, but it depends on the wave geometry. An increase of the Reynolds number, has the consequence of an increase in vortex size and strength of recirculation. Nevertheless, the main part of the stream passes above the vortex without being affected by the reversed flow. Due to its presence, the vortex affects the film thickness. On the first part of the furrow, the film thickness stays constant until the vortex position. At the vortex location the film thickness grows and reaches a maximum at the vortex centre. Afterwards the film thickness decreases until its initial constant value. As the recirculation zone increases with the Reynolds number, the film thickness does the same. The steady behaviour is kept all along the laminar flow range, i.e.  $Re \leq 300$ . Hereafter, the flow becomes turbulent and the vortex has an unsteady motion.

Concerning heat and mass transfer results, the mean Nusselt number at the wall and the mean Sherwood number at the interface are evaluated for one furrow and compared to the smooth surface. Fig. 3 represents the comparison between the mean Sherwood numbers for both surfaces, and it shows that there is a little enhancement for the wavy wall. As the recirculation zone does not directly touch the interface, because its maximum size is not important enough, the mean Sherwood number is quite the same for both surfaces. The interface neighbourhood where the concentration gradient is situated, is not renewed by the vortex. At the beginning of the laminar flow, the ratio is greater than one because of the increase of the exchange area in the case of the wavy wall. At the end of this regime, the slight increase can be attributed to heat transfer enhancement.

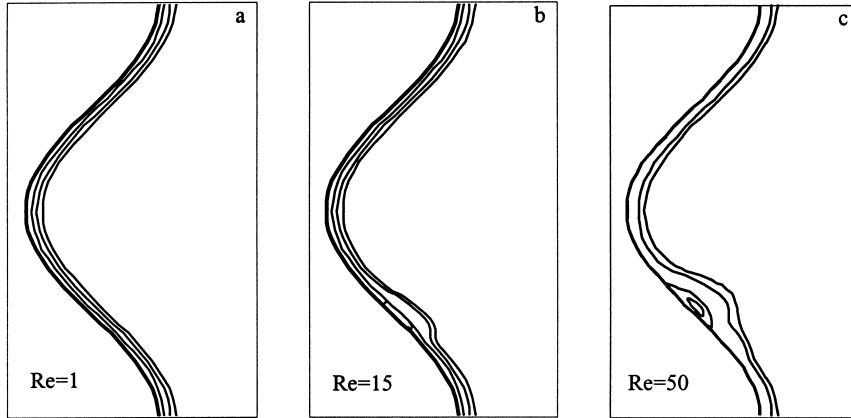


Fig. 2. Stream lines for various  $Re$ .

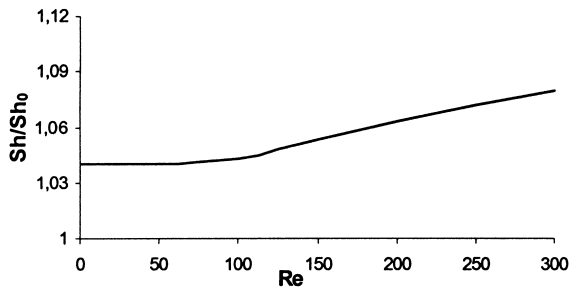


Fig. 3. Comparison of the Sherwood numbers.

For heat transfer, the increase is higher and the more intense the vortex, the more the ratio increases, Fig. 4. The curve can be decomposed into three phases. First, a constant ratio until the vortex formation (1). Then phases (2) and (3), where the enhancement is accomplished in two steps which correspond to the phase of vortex intensification. The vortex is responsible for the heat transfer increase. With the reverse flow the thermal boundary layer is cut off and renewed with fresh liquid of the main stream. When the Reynolds number is enhanced, the vortex becomes more intense, and as a consequence, the heat transfer increases.

A more precise interpretation of enhancement of transfers due to flow pattern can be accomplished by the analysis

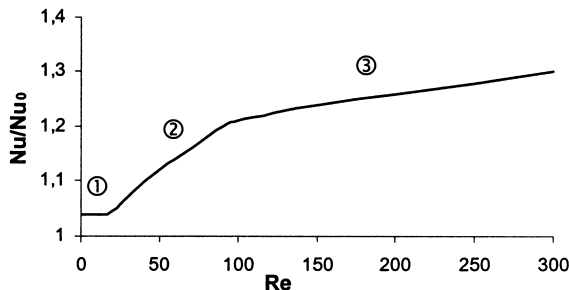


Fig. 4. Comparison of the Nusselt numbers.

of the local heat and mass transfer coefficients. It is not the purpose here, but it has been done in [8]. Before simulating an entire column, an experimental validation is needed. It concerns hydrodynamics, as all results depend on the flow pattern. The set-up is a closed hydrodynamic loop consisting of a test section, a receiving tank, a centrifugal pump and an electrical pre-heater in order to ensure constant temperature and fluid properties. The test section is composed of 31 furrows; each is 22 mm long and 8 mm deep. To appraise the film thickness, an optical method, composed of a CCD video camera connected to an image treatment software package, is used. This software package gives a complete range of functions for treatment, analysis and interpretation of shots. The experimental and theoretical results are compatible: interface position, vortex location (Fig. 5), film thickness (Fig. 6). Fig. 5 represents the position of two particular points: the separation point S, where the flow starts to leave the wall, and the reattachment point R, where it reattaches itself to the wall. The ratio between the experimental and theoretical thickness is shown on Fig. 6. There is a good agreement between both thicknesses until  $Re = 250$ . After this value of the Reynolds number, the difference becomes important due to the transition to the

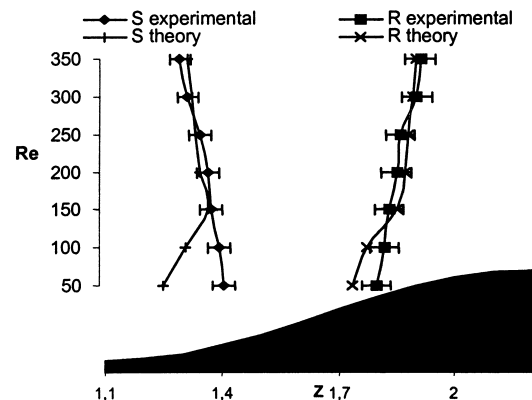


Fig. 5. Comparison of the vortex position.

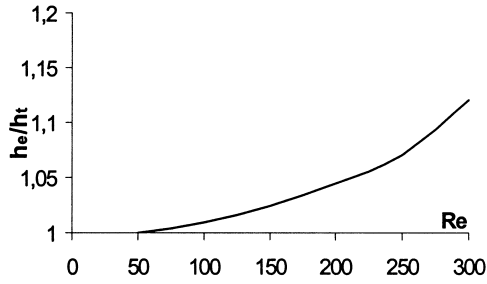


Fig. 6. Comparison of the film thickness.

turbulent flow regime. During the laminar flow, this ratio increases steadily as in the experimental case very small ripples flow over the interface, enhancing the film thickness. The greater the Reynolds number, the more the ripples are important in size. Consequently, this validation leads to the exploitation of the model in the case of a column.

### 3. Modelling of a column

#### 3.1. Model

As explained in the introduction, the simulations were performed for  $\text{SO}_2$  absorption by a falling film of E181. The geometrical characteristics of the column are stated in Table 1. At the inlet, the film flow corresponds to a Reynolds number of 250. The absorption is not important enough to increase the flow rate up to  $Re = 300$ , where the turbulent flow regime starts. At the inlet, the E181 is completely pure, and at the temperature of 293 K. The gas phase is supposed to be pure (only  $\text{SO}_2$ ) and at 293 K as well. The wall temperature is kept constant all along the column, at 293 K.

After the description of the conditions of simulation, the model presented above for one furrow must be extended to an entire column, i.e. various furrows. For the model written for one furrow, effects of heat and mass transfer on hydrodynamics are neglected due to a short wavelength, but this assumption loses its validity for an entire column. The problem is to take into account the effect of heat and mass transfer on hydrodynamic for an entire column. To solve this requirement, the column is simulated wave after wave with the process presented on Fig. 7. First the hydrodynamic model is solved and it is followed by the resolution of the heat and mass transfer model. At the end of the wave, the mean temperature and composition of the film are calcu-

Table 1  
Geometrical characteristics

|                        |                       |
|------------------------|-----------------------|
| Mean radius ( $r_m$ )  | $20 \times 10^{-2}$ m |
| Wave length ( $p$ )    | $20 \times 10^{-3}$ m |
| Wave amplitude ( $a$ ) | $5 \times 10^{-3}$ m  |
| Number of waves        | 50                    |
| Column length          | 1 m                   |

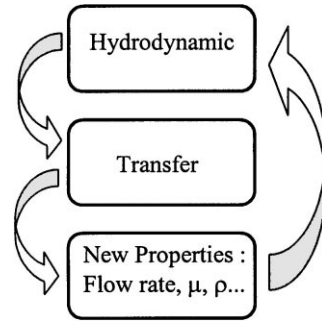


Fig. 7. Calculation Process of a column.

lated in order to evaluate the new flow rate and values of all the fluid properties: viscosity, surface tension. . . The hydrodynamics of the following wave are simulated with the new fluid properties and with the same method. This way to proceed allows to account for the heat and mass transfer effects.

For a single wave, our way to initialise is to use the wave amplitude as a homotopic parameter. As the column is simulated wave after wave, if we preserve this way to initialise, the CPU time cost will be very important. In order to reduce this cost, the initialisation strategy is improved in the case of a whole column. The initialisation of the first column furrow stays as before, i.e. the wave amplitude is gradually increased. For the waves 2 to N, variables are initialised directly for the final furrow geometry (amplitude is not gradually increased) with the results of the preceding furrow, as variables do not evolve in a very important manner.

#### 3.2. Results for a whole column

In order to see the efficiency of the wavy wall column, the column with a smooth wall is simulated under the same operating and geometrical conditions.

Firstly, let us examine the mean film temperature along the wavy and smooth columns, Fig. 8. The absorption is very exothermic, the mean film temperature increased for both surfaces, in spite of wall heat dissipation. The mean temperature of the smooth column is greater than for the wavy wall. As a consequence, the heat transfer rate at the wall is increased in the case of the wavy column as it can be

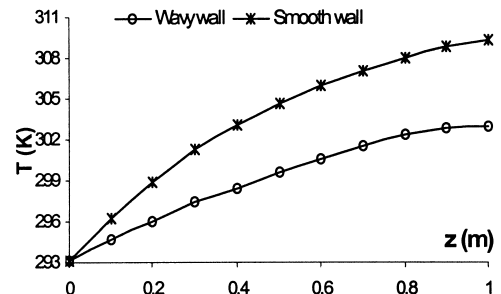


Fig. 8. Mean film temperature.

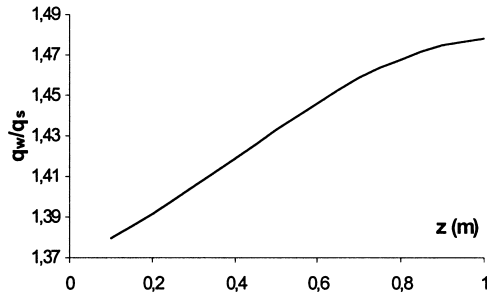


Fig. 9. Ratio of the heat flux at the wall.

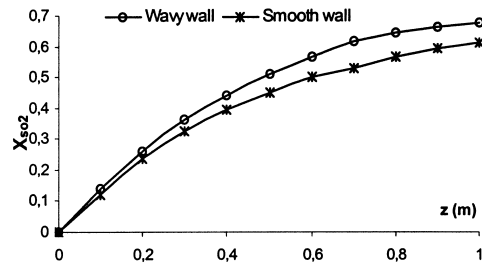


Fig. 10. Mean film composition.

seen on Fig. 9, which represents the ratio of the heat rates at the wall.

At the same time, the mean film composition is greater for the wavy surface, Fig. 10, because the absorption rate increased due to heat transfer, as explained previously. On the first furrows the mean film compositions enhance rapidly. E181 is pure at the inlet therefore  $\text{SO}_2$  is absorbed quickly. Fig. 11 shows the ratios of the mass rates at the interface for both surfaces. On the first part of the column (80 cm), the wavy surface absorbs more  $\text{SO}_2$ . Even if the mass rate is enhanced, the increase of temperature is lower for the wavy wall surface, owing to the heat dissipation at the wall. This heat dissipation is a consequence of the vortex. So specific hydrodynamic conditions directly affect heat transfer and indirectly mass transfer. In fact, the mass transfer is enhanced by heat transfer.

For the last 20 cm of the wavy column, the mean film temperature seems to be stabilised, even though it does continue to increase for the smooth wall. Therefore, there is a

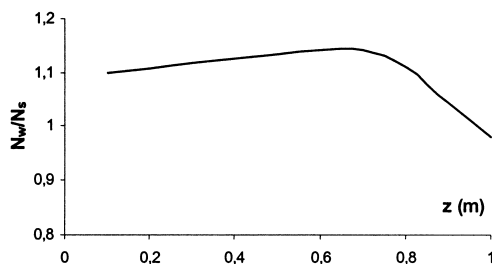


Fig. 11. Ratio of the mass flux at the interface.

less important increase of the dissipated heat flux at the wall for the end of the wavy column, Fig. 8. Moreover, the mean  $\text{SO}_2$  composition stabilises as well for the wavy wall. We can thus conclude that equilibrium is reached for this wall geometry and gas phase condition. For the smooth wall, the mean  $\text{SO}_2$  composition continues to increase, as a consequence the ratio of the interfacial mass flux decreases for the last 20 cm (for the wavy wall the interfacial mass flux does not exist as the equilibrium is reached, consequently the mass transfer across the interface is very small). Finally, for this absorption, the heat transfer increase reaches 43% in favour of the wavy column and it allowed to regulate the temperature absorption. The mass transfer is enhanced too: 10% with a maximum at 12% for the first 80 cm. The second advantage is that equilibrium is reached more rapidly for the wavy column in spite of a lower film temperature.

#### 4. Conclusion

The model considers the laminar flow, heat and mass transfer of a falling film flowing over a wavy wall column. First it is presented for one wave, and the hydrodynamic part is experimentally validated. Then it is extended to an entire column. Because of the particular hydrodynamics, there is a great enhancement of heat transfer at the wall with respect to the smooth surface. A vortex arises in the second part of the wave and cuts off the thermal boundary layer, increasing the heat dissipation. This increase in heat transfer, enhances the mass transfer but in a less important manner. Therefore, the wavy wall column can be used in operations with high heat exchange capacities, as in evaporation, condensation, absorption which necessitate temperature regulation, in gas purification due to their great capacity of treatment.

This numerical investigation concerns laminar flow, it shows that an increase of the transfer exists. The turbulent flow regime is one of our future preoccupations because in this flow regime, the vortex size and strength are more important and heat transfer is greatly affected. The vortex size is able to reach the interface and create the renewal of the concentration boundary layer, and therefore to increase mass transfer.

The gas phase is our next subject of preoccupation. The contribution of the gas phase leads to another amelioration of transfer because of a vortex in this phase. This contribution will be introduced in order to reach a more realistic modelling.

#### References

- [1] Miller, Perez-Blanco, Vertical-tube aqueous LiBr falling film absorption using advanced surfaces, AES 31, International Absorption Heat Pump Conferences ASME (1993) 185–202.
- [2] Sciamanna, Lynn, Solubility of hydrogen sulfide, sulfure dioxide, carbon dioxide, propane, and *n*-butane in poly(glycol ethers), Ind. Eng. Chem. Res. 3 (27) (1988) 492–504

- [3] Slattery, *Interfacial Transport Phenomena*, Springer, New York, 1990.
- [4] Negny, Meyer, Prevost, Simulation of velocity fields in a falling film with a free interface flowing over a wavy surface, *Comput. Chem. Eng.* 22 (1998) S921–S924.
- [5] Prophy, Notice technique, Toulouse (1993).
- [6] Taylor, Krishna, *Multicomponent Mass Transfer*, Wiley, New York, 1983.
- [7] Panday, Laminar film condensation of turbulent vapour flowing inside a vertical tube, in: *Proceedings of the Second International Symposium on Condensers and Condensation*, University of Bath., 1990, pp. 473–482.
- [8] Negny, *Modélisation et étude expérimentale d'un film liquide laminaire à interface libre ruisselant sur une surface structurée: couplage hydrodynamique-transferts de masse et d'énergie*, Thesis INP-ENSIGC, Toulouse, France, 1999.